ACS OMEGA

http://pubs.acs.org/journal/acsodf

Article

Tuning the Energetic Performance of CL-20 by Surface Modification Using Tannic Acid and Energetic Coordination Polymers

Bin Yuan, Yu Zhang, Ke-xin Wang, Tian-ping Wang, Yan Li,* Shun-guan Zhu, Lin Zhang, Zhen-xin Yi, Hua Guan, and Chen-guang Zhu

Cite This: *ACS Omega* 2022, 7, 10469−10475

Read Online

ACCESS | Metrics & More | Article Recommendations | Supporting Information

ABSTRACT: The energetic performance of hexanitrohexaazaisowurtzitane (CL-20) was modulated with two energetic coordination polymers (ECPs), $[Cu(ANQ)_2(NO_3)_2]$ and $[Ni(CHZ)_3](ClO_4)_2$, in this study by a two-step method. First, tannic acid polymerized in situ on the surface of CL-20 crystals. Then, $[Cu(ANQ)_2(NO_3)_2]$ and $[Ni(CHZ)_3](ClO_4)_2$ were hydrothermally formed on the surface of CL-20/TA, respectively. Explosion performance tests show that the impact sensitivity of the coated structure CL-20/TA/$[Cu(ANQ)_2(NO_3)_2]$ is 58% less than that of CL-20 with no energy decrease. On the other hand, CL-20/TA/$[Ni(CHZ)_3](ClO_4)_2$ can be initiated by a low laser energy of 107.3 mJ (Nd:YAG, 1064 nm, 6.5 ns pulse width), whereas CL-20 cannot be initiated by even 4000 mJ laser energy. This study shows that it is feasible to modify the performance of CL-20 by introducing energetic CPs with certain properties, like high energy insensitive, laser-sensitive, etc., which could be a prospective method for designing high energy insensitive energetic materials in the future.

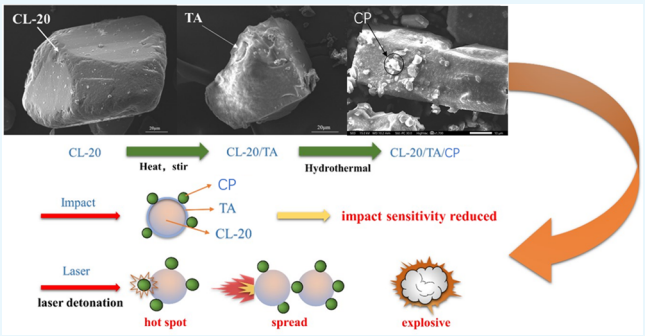

1. INTRODUCTION

In modern military, detonators are generally used to detonate explosives, and commonly used detonators consist of detonating charges and explosives. Laser detonation uses a special method of energy conduction that is much more efficient than conventional detonators and electrical detonators. At the same time, laser detonation has a strong anti-interference ability, high temperature, and pressure resistance, so laser detonation compared to other traditional detonation has safer, more reliable characteristics.[1,2] Laser detonation in detonators is primarily achieved by introducing a sufficiently powerful laser pulse directly onto the surface of an insensitive explosive and specific agents respond to the laser pulse at different wavelengths.[3,4] The laser starting threshold of traditional lead azide is the lowest, but due to its high sensitivity,[5,6] the safety of use cannot be guaranteed. Therefore, the preparation of explosives that can be used directly in laser pulse detonation has become an important direction for the study of laser detonation agents. Part of the study focuses on the doping of RDX/PETN explosives with metal particles such as carbon black and nano-Al,[7,8] due to the high photothermal conversion efficiency of carbon black and nano-Al particles;[9,10] the doped explosives can be directly detonated by laser pulses. But due to the shortcoming of PETN of high mechanical susceptibility, there is a need to explore new means of explosives to prepare laser detonation explosives.

As a typical ammonium nitrate explosive, hexanitrohexaazaisowurtzitane (CL-20) has been used in a variety of artillery shells and propellants in military applications.[11] However, CL-20 is relatively sensitive[12] to impact, and its low light absorption efficiency means the requirement of an ultrahigh laser ignition threshold. There are only few reports on the laser initiation of CL-20 composites. Li et al.[13] used a prolonged high-power laser (8 W, 500 ms, 1064 nm) to initiate CL-20 powder, but it basically only burned at the irradiation point and could not keep burning. It is reported in several studies that CL-20-based thin films, doped with GO, which has a high photothermal conversion efficiency as well as nano-Al,[10,14] could be initiated by laser. Since laser detonation is safer and more reliable than other traditional detonation methods, it is of great research value to study the laser potential initiation ability of the CL-20 composite to possibly replace lead azide.

In recent years, some energetic coordination polymers (ECPs) have been reported to have high energy, high density, low sensitivity, and excellent laser sensitivity. The well-defined

Received: December 25, 2021
Accepted: March 4, 2022
Published: March 16, 2022

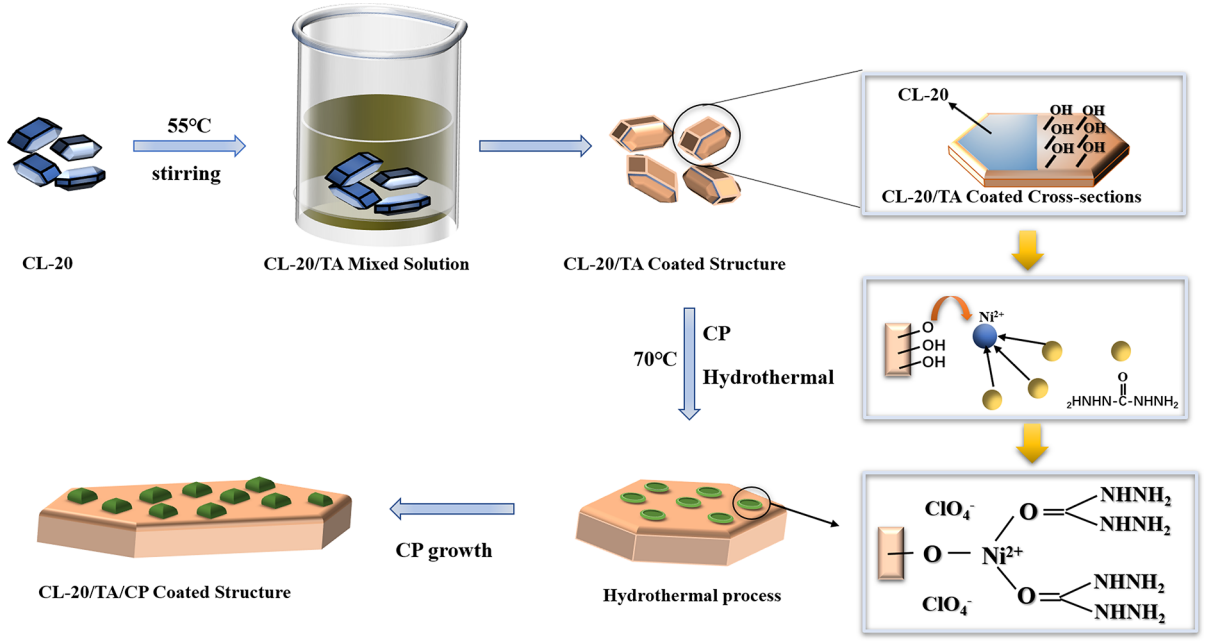

Figure 1. Schematic diagram of the preparation of CL-20/TA/CP, the molecular formula of tannic acid, and the binding site of CL-20/TA to Ni^{2+} and carbonyls.

skeletal structure of ECPs makes it possible to modify high-energy sensitive explosives, like CL-20, with CPs of certain characteristics;[15−18] specifically because the lower sensitivity of most ECPs is evaluated relative to the primary explosives, it is possible to adjust the sensitivity of high energy explosives. So, the question arises as to how the explosives can be connected to the CPs. Coating as a basic means of modifying energy-containing materials is simply the use of some high-energy explosives, high-energy binders, and some passivating agents to coat energy-containing materials at the microscopic level, so that the impact sensitivity or friction and other sensitivities of the explosive are reduced and can be used to prepare low-sensitivity, high-energy materials.[19−21] The combination of CL-20 and CPs using a coated structure also may serve the purpose of adjusting the sensitivity of CL-20 composites.

In this study, CL-20 is modified by a two-step procedure, as is shown in Figure 1. In the first step, the CL-20 particle is coated with a self-polymer tannic acid (TA). In the second step, $[Cu(ANQ)_2(NO_3)_2]$ (CP 1) and $[Ni(CHZ)_3](ClO_4)_2$ (CP 2) are produced according to the method described in the literature,[22,23] and then CP is crystallized perfectly on top of CL-20/TA by the hydrothermal reaction at high temperature and pressure. By these two steps, we can obtain the structure of CL-20/TA/CP.

The selection of tannic acid as the coating of CL-20 is because there are many hydroxyl groups around TA molecules the can grab the polymer chain through the hydrogen bond and ionic bond and cross-link the polymer chains through the coordination bond in the presence of metal ions.[24] As shown in Figure 1, under hydrothermal conditions, the metal ions will form coordination bonds with the carbonyl oxygen of the ligand, and the hydroxyl oxygen of tannic acid will also coordinate with the metal ions to form an induced effect. This leads to the growth of CP on the surface of tannins, and the coating effect of tannic acid also reduces the sensitivity of CL-20.

To solve the problem of energy loss after CL-20 encapsulation, the selection of CP also needs to be considered. CPs have different properties, and one point of concern here is that CP containing perchlorate can be used for laser ignition or laser detonation. CP 1, an energy-containing CP with higher performance, was chosen to reduce the CL-20 susceptibility without energy loss.[22] CP 1 is composed of amino-nitro-guanidine (ANQ) as an energy-containing ligand and copper as a coordination metal ion, and another ligand as the nitrate ion. CP 2, consisting of carbonyl hydrazine (CHZ) as an energy-containing ligand, nickel as a coordination metal ion, and another ligand as a perchlorate ion, is capable of laser detonation[23] and was chosen with the hope that CL-20 could be directly detonated by a laser after treatment.

2. MATERIALS AND METHODS

2.1. Materials and Instruments. ε-CL-20 (Analytical Pure, Nanjing University of Science and Technology), copper nitrate hydrate (99%, Aladdin), anhydrous ethanol (99.7%, Sin pharm Chemical Reagent Co., Ltd.), carbohydrazide (97%, Aladdin), guanidine nitrate (Nanjing University of Science and Technology), concentrated sulfuric acid (98%, Nanjing Sheng Qing He Chemical Co., Ltd.), hydrazine hydrate (85%, Aladdin), nickel perchlorate hexahydrate (99%) (Aladdin), and tannic acid (95%, Aladdin) were used.

Scanning electron microscopy (SEM) photographs were obtained by a Nihon Kohen JSM-IT500HR scanning electron microscope. X-ray diffraction (XRD) measurements were carried out on Bruker X-ray Fluorescence D8 ADVANCE. X-ray photoelectron spectroscopy (XPS) was carried out on a PHI Quan tera II photoelectron spectrometer. Infrared spectroscopy (IR) was measured on a Nicolet IS10 FTIR spectrometer. Differential scanning calorimeter (DSC) and thermogravimetric analysis (TG) was used to study the thermal decomposition process on a Mettler DSC 823e differential scanning calorimeter and a Mettler Toledo TGA SDTA851 thermogravimetric analyzer, respectively.

https://doi.org/10.1021/acsomega.1c07282
ACS Omega 2022, 7, 10469−10475

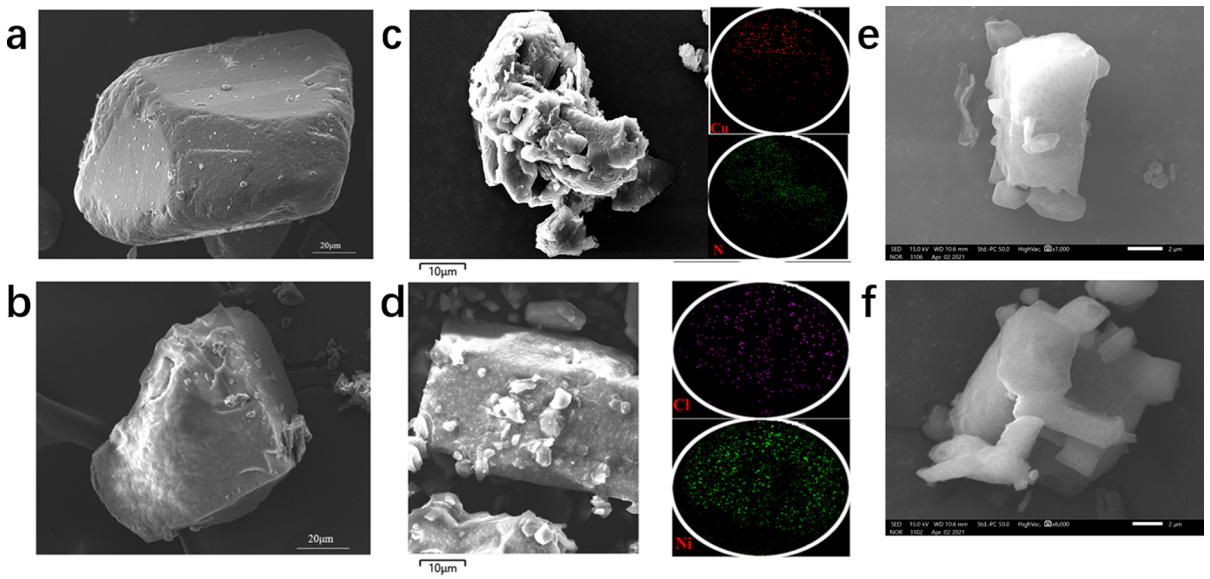

Figure 2. SEM of CL-20 and CL-20/TA and EDS of CL-20/TA/CP. (a) SEM image of CL-20. (b) SEM image of CL-20/TA. (c) SEM and EDS images of CL-20/TA/CP 1. (d) SEM and EDS images of CL-20/TA/CP 2. (e) SEM image of CP 1. (f) SEM image of CP 2.

2.2. Preparation of 3-Amino-1-nitroguanidine (ANQ). The preparation of 3-amino-1-nitroguanidine (ANQ) involves two major steps. First, 20 g of guanidine nitrate was added to 30 mL of concentrated sulfuric acid in a beaker, and the solution was cooled to 0 °C. Then, the beaker was taken out and stirred for 20 min, at room temperature. Subsequently, the sample was slowly poured into 300 mL of iced water. Then a large number of white nitroguanidine crystals precipitated, and they were filtered and dried. The yield was 72.3%.

Then, 25 g of nitroguanidine was added to 250 mL of water, and the solution was heated to 55 °C; then, 10.5 mL of hydrazine hydrate was added for 15 min, with continued stirring of the solution for another 15 min. After cooling to room temperature, hydrochloric acid was added, and the solution was kept at 4 °C for 12 h.[22]

2.3. Preparation of CP. *2.3.1. CP 1.* 3-Amino-1-nitroguanidine (0.50 g) was dissolved in 20 mL of water, and the solution was heated to 70 °C and stirred. Copper(II) nitrate trihydrate (1.02 g) was added, and the mixture was heated until it became clear. The clear solution was filtered and slowly cooled to room temperature. After 1 h, the product started to crystallize as deep blue crystals. Yield: 15%.[22]

2.3.2. CP 2. 1,3-Diaminomocovina (0.50 g) was dissolved in 20 mL of 55 °C water. Then nickel(II) perchlorate hexahydrate (2.02 g) was added. When the clear solution slowly cooled to room temperature. The product started to crystallize as deep blue crystals.[23]

2.4. Preparation of CL-20/TA/CP. Preparation of CL-20/TA/CP was carried out by two steps. First, 100 mg of tannic acid was dissolved in 300 mL of water, and 1 g of CL-20 was added and stirred while the solution was heated to 50 °C and kept for 4 h, filtered, and dried. Then, 200 mg of the above prepared CP was dissolved in 20 mL of heated solution of 20% ethanol with water, and 1 g of CL-20/TA was added. The resulting solution was reacted in a hydrothermal reactor at 70 °C. After 24 h, the solution was filtered and dried with a yield of 89%.

3. RESULTS AND DISCUSSION

3.1. Characterization of CL-20/TA/CP. Figure 2a–f shows SEM of CL-20, CL-20/TA, CP 1, and CP 2 and SEM and EDS of CL-20/TA/CP 1 and CL-20/TA/CP 2, respectively. CL-20, which is the highest-energy crystal type among four crystal types of CL-20,[25] was used in this study. Compared with the smooth surface of pure CL-20, the surface of CL-20/TA is rougher as is shown in Figure 2b. At the same time, an extra layer of film-like material can be seen on the surface, which indicates that TA smoothly wraps around the crystal surface of CL-20. Figure 2c,d shows the SEM image of CL-20/TA/CP as well as the EDS image, which shows many small crystals outside the cladding layer. It can be assumed that CPs grow on the surface of CL-20/TA. Figure 2e,f show the SEM of CP 1 and CP 2.

The presence of TA on the surface of CL-20 was then confirmed by FTIR measurement. It can be seen from Figure 3 that both CL-20 and CL-20/TA have sharp absorption peaks

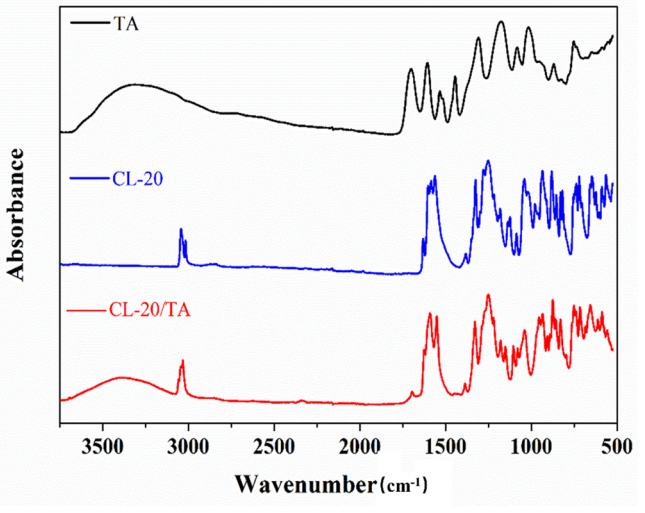

Figure 3. FTIR spectra of TA, CL-20, and CL-20/TA.

https://doi.org/10.1021/acsomega.1c07282
ACS Omega 2022, 7, 10469−10475

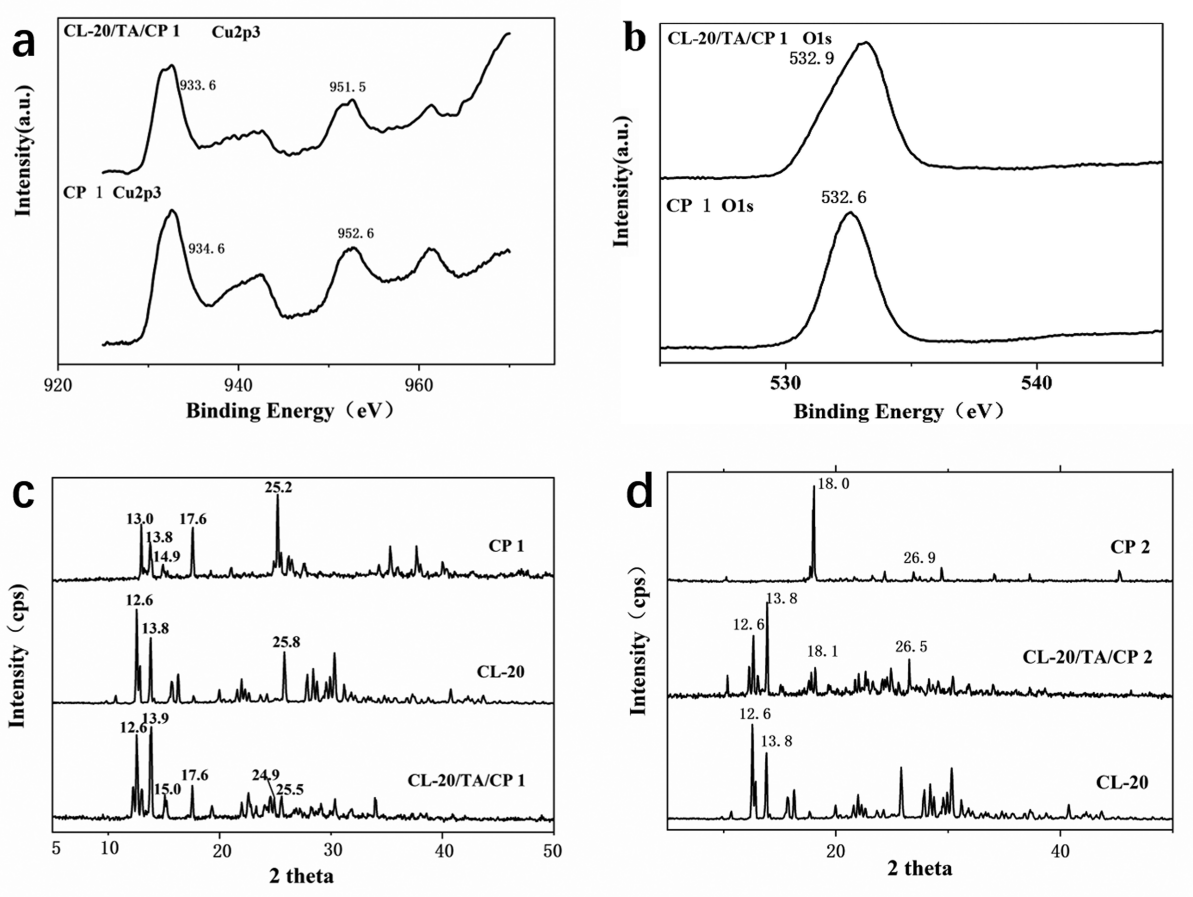

Figure 4. XPS and XRD of CL-20/TA/CP. (a) XPS spectra of O 1s of CP 1 with CL-20/TA/CP 1. (b) XPS spectra of Cu 2p3 of CP 1 with CL-20/TA/CP 1. (c) XRD spectra of CP 1, CL-20/TA/CP 1, and CL-20. (d) XRD spectra of CP 2, CL-20/TA/CP 2, and CL-20.

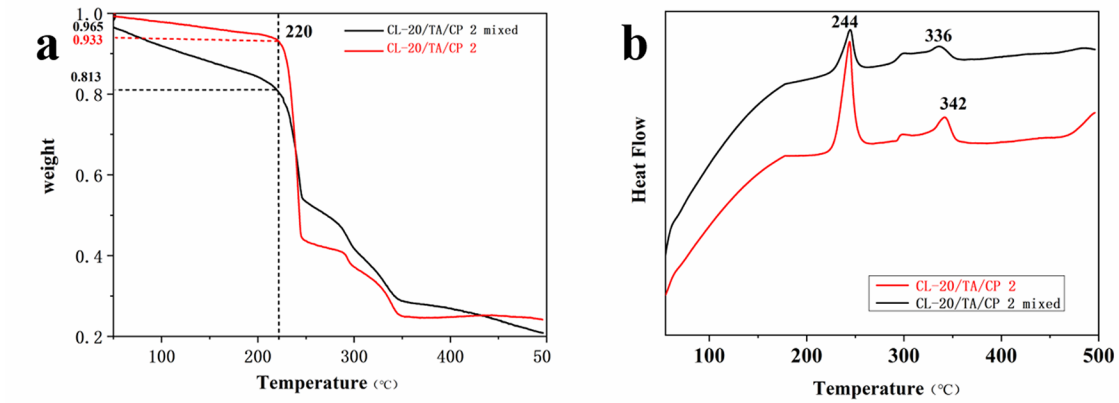

Figure 5. TG and DSC curves of CL-20/TA/CP 2. (a) TG curves of CL-20/TA/CP 2 and CL-20/TA/CP 2 mixtures. (b) DSC curves of CL-20/TA/CP 2 and CL-20/TA/CP 2 mixtures.

at 3050 cm^{-1}, which is the stretching vibration absorption peak of C−H bonds. At 1590 cm^{-1}, an absorption peak of $-NO_2$ appeared, indicating the presence of CL-20. The stretching vibration of the lipid C═O at 1700 cm^{-1} indicates that TA has self-polymerized, which is also approved by the previous SEM image. It can be concluded that TA self-polymerizes on the CL-20 surface.

Figure 4a shows the XPS spectra of Cu 2p3 of CP 1 and CL-20/TA/CP 1. The Cu 2p3 of CP 1 has characteristic peaks at 934.6 and 952.6 eV and a significant shoulder peak of Cu(II) species at 934.0 eV; due to the coordination of Cu with carbonyl oxygen in CP 1, the binding energy of Cu with carbonyl oxygen is changed. The Cu 2p3 of CL-20/TA/CP 1 has characteristic peaks at 933.6 eV, 934.6 eV, 951.5 eV, and 952.6 eV, and some of these peaks are the same as those of CP 1, indicating Cu as a CP structure in sample CL-20/TA/CP 1. At the same time, the binding energy of Cu decreased to 933.6 and 951.5 eV due to the increase in the electron cloud density

https://doi.org/10.1021/acsomega.1c07282
ACS Omega 2022, 7, 10469−10475

around Cu after TA involvement in coordination; the oxygen peaks become more numerous, and the binding energy increased, both due to the addition of hydroxyl oxygen (532.3 eV) and the change in electron cloud density. Figure 4b shows the XPS spectra of O 1s of CP 1 and CL-20/TA/CP 1. The O 1s of CL-20/TA/CP 1 has characteristic peaks at 532.9 and 533.2 eV. The O 1s of CP 1 has characteristic peaks at 532.6 eV and carbonyl oxygen characteristic peaks at 532.8 eV.

In Figure 4c, powder X-ray diffraction (PXRD) shows that the main characteristic peaks of CL-20 are 12.6°, 13.8°, and 25.8°, which correspond to the XRD of the epsilon crystal type. CL-20/TA/CP 1 also has these characteristic peaks at the same diffraction angels, indicating that ε-CL-20 did not undergo transmutation during the preparation steps. The characteristic peaks of CP 1 at 14.9°, 17.6°, and 25.2° also exist in the XRD spectrum of CL-20/TA/CP 1, indicating the presence of CP 1 in CL-20/TA/CP 1, further proving the presence of copper elements is in the form of the CP structure. Similarly, in Figure 4d, ε-CL-20 did not undergo transmutation, and at the same time, the characteristic peaks of CP 2 at 10.2°, 18.0°, and 26.9° can be found in the XRD spectrum of CL-20/TA/CP 2, indicating the presence of CP 2 in CL-20/TA/CP 2.

The above characterizations of the samples were done to prove that the conjecture of this structure of CL-20/TA/CP is correct and feasible.

3.2. Thermal Stability of CL-20/TA/CP 2. For high explosives, safety is a priority, both in terms of sensitivity and thermal stability; an important purpose of the CL-20/TA/CP structure is also to reduce sensitivity while ensuring good thermal stability. In Figure 5, TG-DSC tests were performed on CL-20/TA/CP 2 and CL-20/TA/CP 2 mixtures in order to compare the thermal stability of CL-20/TA/CP 2 with mechanical mixtures (CL-20/TA/CP 2 mixture). As shown in Figure 5a, the weight of the CL-20/TA/CP 2 mixture decreased about 15.2%, while that of CL-20/TA/CP 2 decreased about 6.4% during the temperature increase from 50 to 220 °C, indicating that the decomposition of tannic acid is delayed after self-polymerization. Overall, CL-20/TA/CP 2 is a structure with good thermal stability. The first exothermic peak of CL-20 is at 244 °C (Figure 5b), which is essentially unchanged. Another peak at 336 °C is the CP 2 exothermic peak in the CL-20/TA/CP 2 mixture, but CL-20/TA/CP 2 is slightly delayed to 342 °C. It is illustrated that the reaction process is unchanged after mixing and coating, but the decomposition of CP 2 is slightly delayed, possibly due to the effect of TA involvement in coordination.

3.3. Explosion Performance of CL-20/TA/CP 1. The impact sensitivity of CL-20/TA/CP 1 as well as that of CL-20 was tested by the drop-weight test, as is shown in Table 1. Compared with that of pure CL-20, the impact sensitivity of CL-20/TA/CP 1 decreased by 58%, which might be caused by the polymerization of tannic acid on the surface of CL-20. The detonation velocity of CL-20 is determined by an electrical method (pin oscillographic Technique). The main explosive charge (3 g, 70 MPa) is pressed into a 6 mm diameter detonator, and the distance between the two probes is 40 mm. As is shown in Table 1, the detonation velocity of CL-20 is 7500 m·s^{-1} (ρ1 = 1.938), while the detonation velocity of CL-20/TA/CP 1 (ρ1 = 1.845) is 7312 m·s^{-1}, according to the Kamlet−Jacobs equation. When CL-20/TA/CP 1 has the same density as CL-20, the detonation velocity is 7466 m·s^{-1}, which means there is almost no difference in detonation velocity after surface modification.

Table 1. Explosion Performance Test Results of CL-20 and CL-20/TA/CP 1[a]

sample	ρ_0 (g·cm^{-3})	H_{50} (cm)	DV (m·s^{-1})	ρ_1 (g·cm^{-3})
CL-20	2.040	12	7500	1.938
CL-20/TA/CP 1	1.982	19	7312	1.845

[a] ρ_0: theoretical density, H_{50}: 2.5 kg drop hammer, 50% firing drop height, DV: detonation velocity, ρ_1: pressure charge density.

To further prove that the outermost [Cu(ANQ)$_2$(NO$_3$)$_2$] can compensate for the energy loss associated with the impact sensitivity decrease by TA, 6 mm diameter detonators filled with detonating explosive (nickel hydrazine azide, 70 mg), booster explosive (hexogen, 200 mg), and main explosive charges (CL-20, the CL-20/TA/CP 1 mixture, and the CL-20/TA/CP 1 mixture, 500 mg) were used to do the lead plate (5 mm depth) experiment. The bore diameters with CL-20, the CL-20/TA/CP 1 mixture (twice), and the CL-20/TA/CP 1 mixture as main explosives are 11 mm, 9.8 mm, 10.3 mm, and 9 mm, respectively (Figure 6). It can be concluded that the explosive performance of CL-20/TA/CP 1 is better than that of the CL-20/TA/CP 1 mixture despite the energy loss. Overall, the surface modification of CL-20 with TA and CP 1 achieves the purpose of reducing the impact sensitivity of CL-20 without losing too much energy.

3.4. Laser Detonation of CL-20/TA/CP 2. As [Ni(CHZ)$_3$](ClO$_4$)$_2$ (CP 2) has good laser sensitivity, the laser ignition performance of CL-20/TA/CP 2 was evaluated by a device consisting of a solid pulsed laser (1064 nm, 6.5 ns), a K9 sapphire glass window, a charging chamber, and a rear lead plate. The laser beam passed through a sapphire window and irradiated on the surface of CL-20/TA/CP 2. High-speed photography (40 000 fps) was used to detect the blasting phenomenon.

A total of 20 mg of CL-20/TA/CP 2 was charged in a detonator with a diameter of 5 mm and a height of 2 mm and was initiated by a laser energy of 107.3 mJ. As shown in Figure 7, initiation of the CL-20/TA/CP 2 begins at 5 μs, and complete detonation happens at 30 μs; the detonation ends after 55 μs. The experiment shows that CL-20/TA/CP 2 is laser ignitable. Whereas, the CL-20/TA/CP 2 mixture cannot be ignited with even higher energy (1064 nm, 4000 mJ), which further proves that the outside [Ni(CHZ)$_3$](ClO$_4$)$_2$ greatly improves the laser sensitivity of CL-20.

Figure 8 shows the schematic diagram of the laser detonation experiments. The charging sequence is 200 mg of CL-20/TA/CP 2 and 500 mg of CL-20; the detonator diameter is 6 mm, and the thickness of the lead plate is 5 mm. As shown in Figure 8b, the lead plate explosive aperture is 8.5 mm, which is 2.5 mm larger than the detonator diameter, indicating that CL-20/TA/CP 2 is fully detonated.

4. CONCLUSIONS

In this work, we designed a coated structure modified hexanitrohexaazaisowurtzitane (CL-20), a high-energy explosive. First, to reduce the sensitivity of CL-20, a self-polymerizable organic material tannic acid (TA) was utilized to coat the surface of CL-20. Second, two energetic metal complexes were used, CP 1, [Cu(ANQ)$_2$(NO$_3$)$_2$, and CP 2, [Ni(CHZ)$_3$](ClO$_4$)$_2$. CP 1 is a high energy explosive, and CP 2 can be used as a laser detonation agent. Characterization of

https://doi.org/10.1021/acsomega.1c07282
ACS Omega 2022, 7, 10469−10475

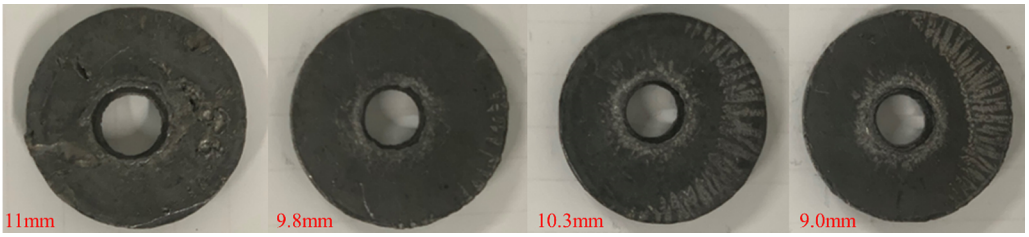

Figure 6. CL-20, CL-20/TA/CP 1, and CL-20/TA/CP 1 mixture lead plate experiment.

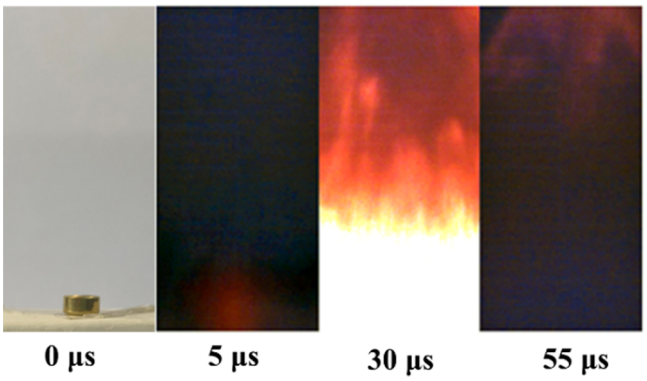

Figure 7. High-speed photography images of laser detonation experiments

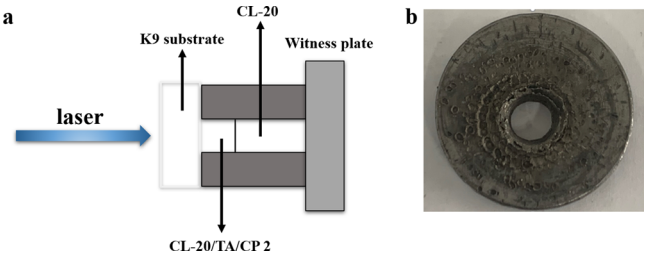

Figure 8. Schematic diagram and laser detonation experiment. (a) Schematic diagram of the laser detonation experiment. (b) Lead plate after the laser detonation experiment.

the prepared samples demonstrated the existence of a coated structure. Tannic acid cover the surface of CL-20. Due to the large number of hydroxyl groups on the tannic acid surface, the metal ions coordinate with the hydroxyl groups, thus promoting the growth of CP on the TA coating layer. Through performance tests and calculations, the impact sensitivity of CL-20 is reduced by 58%, and the energy of CL-20 is reduced by 2.5% compared with that of uncoated CL-20, which achieves the purpose of sensitivity reduction of CL-20 without losing much energy. Moreover, the other coated structure CL-20/TA/CP 2 is capable of laser initiation at 107.3 mJ with a Nd:YAG laser (1064 nm, 6.5 ns) and lead plate test further proving that CL-20/TA/CP 2 is fully detonated. This work obtained high-energy insensitive and laser sensitive CL-20 series explosives by introducing a coated structure surface modification. Due to the diversity and versatility of energetic coordination polymers (ECPs), this study will provide new ideas for the preparation of high-energy insensitive explosives and more possibilities for the modification of imperfect explosives.

■ ASSOCIATED CONTENT

Supporting Information

The Supporting Information is available free of charge at https://pubs.acs.org/doi/10.1021/acsomega.1c07282.

Figure S1, measured and simulated XRD of CP 1; Figure S2, measured and simulated XRD of CP 2; Figure S3, UV−vis−NIR spectra of CP 2 and CL-20/TA/CP 2; Figure S4, DSC spectra of CP 1 and CL-20/TA/CP 1; Figure S5, TG spectra of CP 1 and CL-20/TA/CP 1; Figure S6, diagram of the lead plate experiment and charging sequence for the detonator; and Figure S7, diagram of the laser detonation and high-speed photography experiment (PDF)

■ AUTHOR INFORMATION

Corresponding Author

Yan Li − *School of Chemistry and Chemical Engineering, Nanjing University of Science and Technology, Nanjing 210094, P. R. China;* orcid.org/0000-0003-3483-4970; Email: yanli@njust.edu.cn

Authors

Bin Yuan − *School of Chemistry and Chemical Engineering, Nanjing University of Science and Technology, Nanjing 210094, P. R. China;* orcid.org/0000-0002-6205-8297

Yu Zhang − *School of Chemistry and Chemical Engineering, Nanjing University of Science and Technology, Nanjing 210094, P. R. China*

Ke-xin Wang − *School of Chemistry and Chemical Engineering, Nanjing University of Science and Technology, Nanjing 210094, P. R. China*

Tian-ping Wang − *School of Chemistry and Chemical Engineering, Nanjing University of Science and Technology, Nanjing 210094, P. R. China*

Shun-guan Zhu − *School of Chemistry and Chemical Engineering, Nanjing University of Science and Technology, Nanjing 210094, P. R. China*

Lin Zhang − *School of Chemistry and Chemical Engineering, Nanjing University of Science and Technology, Nanjing 210094, P. R. China;* orcid.org/0000-0002-4193-8877

Zhen-xin Yi − *School of Chemistry and Chemical Engineering, Nanjing University of Science and Technology, Nanjing 210094, P. R. China*

Hua Guan − *School of Chemistry and Chemical Engineering, Nanjing University of Science and Technology, Nanjing 210094, P. R. China*

Chen-guang Zhu − *School of Chemistry and Chemical Engineering, Nanjing University of Science and Technology, Nanjing 210094, P. R. China*

Complete contact information is available at: https://pubs.acs.org/10.1021/acsomega.1c07282

https://doi.org/10.1021/acsomega.1c07282
ACS Omega 2022, 7, 10469−10475

Notes

The authors declare no competing financial interest.

■ ACKNOWLEDGMENTS

This work was supported by the National Natural Science Foundation of China (51676100).

■ REFERENCES

(1) Ahmad, S. R.; Russell, D. A. Laser Ignition of Pyrotechnics - Effects of Wavelength, Composition and Confinement. *Propell Explos Pyrot* **2005**, *30* (2), 131−139.
(2) Du, J. G.; Ma, H. H.; Shen, Z. W. Laser Initiation of Non-Primary Explosive Detonators. *Propell Explos Pyrot* **2013**, *38* (4), 502−504.
(3) Lisitsyn, V.; Morozova, E.; Skripin, A.; Tsipilev, V. Spectral dependence of the initiation threshold of explosive decomposition in AgN_3. *Nucl. Instrum Meth B* **2012**, *286*, 141−147.
(4) Ahmad, S. R.; Russell, D. A.; Leach, C. J. Studies into Laser Ignition of Unconfined Propellants. *Propell Explos Pyrot* **2001**, *26*, 235−245.
(5) Ugryumov, I. A.; Ilyushin, M. A.; Tselinskii, I. V.; Kozlov, A. S. Synthesis and Properties of Photosensitive ComplexPerchlorates of d Metalswith 3(5)-Hydrazino-4-amino-1,2,4-triazole as Ligand. *Russ J. Appl. Chem.* **2003**, *76* (3), 439−441.
(6) Wang, H.; Chu, E.; Hong, J.; He, A.; Cao, C.; Jing, B.; Ma, Y.; Hu, Y. Laser Initiation BNCP Driven by Super Capacitor. *Chin J. Energ Mater.* **2019**, *27* (3), 242−248.
(7) Aduev, B. P.; Nurmukhametov, D. R.; Furega, R. I.; Zvekov, A. A.; Kalenskii, A. V. Explosive decomposition of PETN with nanoaluminum additives under the influence of pulsed laser radiation at different wavelengths. *Russ J. Phys. Chem. B* **2013**, *7* (4), 453−456.
(8) Aluker, É. D.; Belokurov, G. M.; Krechetov, A. G.; Mitrofanov, A. Y.; Nurmukhametov, D. R. Laser initiation of PETN containing light-scattering additives. *Tech Phys. Lett.* **2010**, *36* (3), 285−287.
(9) Jiang, Y.; Deng, S.; Hong, S.; Zhao, J.; Huang, S.; Wu, C.; Gottfried, J.; Nomura, K.; Li, Y.; Tiwari, S.; et al. Energetic Performance of Optically Activated Aluminum/Graphene Oxide Composites. *ACS Nano* **2018**, *12* (11), 11366−11375.
(10) Zhang, X.; Hikal, W. M.; Zhang, Y.; Bhattacharia, S. K.; Li, L.; Panditrao, S.; Wang, S.; Weeks, B. L. Direct laser initiation and improved thermal stability of nitrocellulose/graphene oxide nanocomposites. *Appl. Phys. Lett.* **2013**, *102* (14), 141905.
(11) Vuppuluri, V. S.; Samuels, P. J.; Caflin, K. C.; Gunduz, I. E.; Son, S. F. Detonation Performance Characterization of a Novel CL-20 Cocrystal Using Microwave Interferometry. *Propell Explos Pyrot* **2018**, *43* (1), 38−47.
(12) Bennion, J. C.; Chowdhury, N.; Kampf, J. W.; Matzger, A. J. Hydrogen Peroxide Solvates of 2,4,6,8,10,12-Hexanitro-2,4,6,8,10,12-hexaazaisowurtzitane. *Angew. Chem. Int. Edit* **2016**, *55* (42), 13118−13121.
(13) Li, X.; Huang, B.; Li, R.; Zhang, H.; Qin, W.; Qiao, Z.; Liu, Y.; Yang, G. Laser-Ignited Relay-Domino-Like Reactions in Graphene Oxide/CL-20 Films for High-Temperature Pulse Preparation of Bi-Layered Photothermal Membranes. *Small* **2019**, *15* (20), 1900338.
(14) Su, Y.; Sun, Y.; Zhao, J. Interaction Mechanisms of Insensitive Explosive FOX-7 and Graphene Oxides from Ab Initio Calculations. *Nanomaterials (Basel)* **2019**, *9* (9), 1290.
(15) Ma, X.; Chen, X.; Li, Y.; Qiao, Z.; Yang, G.; Zhang, K. Aluminized Energetic Coordination Polymers Constructed from Transition Metal Centers (Co, Ni, and Cu). *Propell Explos Pyrot* **2021**, *46*, 1598−1610.
(16) Hu, L.; Yin, P.; Zhao, G.; He, C.; Imler, G. H.; Parrish, D. A.; Gao, H.; Shreeve, J. Conjugated Energetic Salts Based on Fused Rings: Insensitive and Highly Dense Materials. *J. Am. Chem. Soc.* **2018**, *140* (44), 15001−15007.
(17) Yang, G.; Li, X.; Wang, M.; Xia, Z.; Yang, Q.; Wei, Q.; Xie, G.; Chen, S.; Gao, S.; Lu, J. Y. Improved Detonation Performance Via Coordination Substitution: Synthesis and Characterization of Two New Green Energetic Coordination Polymers. *ACS Appl. Mater. Inter* **2021**, *13*, 563−569.
(18) Wurzenberger, M. H. H.; Lechner, J. T.; Stierstorfer, J. Copper(II) Dicyanamide Complexes with N-Substituted Tetrazole Ligands - Energetic Coordination Polymers with Moderate Sensitivities. *ChemPlusChem.* **2020**, *85* (4), 769−775.
(19) Yang, Z.; Ding, L.; Wu, P.; Liu, Y.; Nie, F.; Huang, F. Fabrication of RDX, HMX and CL-20 based microcapsules via in situ polymerization of melamine−formaldehyde resins with reduced sensitivity. *Chem. Eng. J.* **2015**, *268*, 60−66.
(20) Yang, Z.; Li, J.; Huang, B.; Liu, S.; Huang, Z.; Nie, F. Preparation and Properties Study of Core-Shell CL-20/TATB Composites. *Propell Explos Pyrot* **2014**, *39* (1), 51−58.
(21) Zhang, X.; Chen, S.; Wu, Y.; Jin, S.; Wang, X.; Wang, Y.; Shang, F.; Chen, K.; Du, J.; Shu, Q. A novel cocrystal composed of CL-20 and an energetic ionic salt. *Chem. Commun. (Camb)* **2018**, *54* (94), 13268−13270.
(22) Fischer, N.; Joas, M.; Klapotke, T. M.; Stierstorfer, J. Transition metal complexes of 3-amino-1-nitroguanidine as laser ignitible primary explosives: structures and properties. *Inorg. Chem.* **2013**, *52* (23), 13791−13802.
(23) Joas, M.; Klapötke, T. M. Laser Initiation of Tris-(carbohydrazide)metal(II) Perchlorates and Bis(carbohydrazide)-diperchlorato-copper(II). *Propell Explos Pyrot* **2015**, *40* (2), 246−252.
(24) Fan, H.; Wang, L.; Feng, X.; Bu, Y.; Wu, D.; Jin, Z. Supramolecular Hydrogel Formation Based on Tannic Acid. *Macromolecules* **2017**, *50* (2), 666−676.
(25) Song, X.; Wang, Y.; An, C.; Guo, X.; Li, F. Dependence of particle morphology and size on the mechanical sensitivity and thermal stability of octahydro-1,3,5,7-tetranitro-1,3,5,7-tetrazocine. *J. Hazard Mater.* **2008**, *159* (2−3), 222−229.

https://doi.org/10.1021/acsomega.1c07282
ACS Omega 2022, 7, 10469−10475